Detection of H^+ recoiled from Si(111)-1×1-H by Medium Energy Ne^+ Impact

K. Mitsuhara, H. Okumura, T. Matsuda, M. Tagami, A. Visikovskiy* and Y. Kido

Department of Physics, Ritsumeikan University, Kusatsu, Shiga-ken 525-8577, Japan

Abstract

We detected the H^+ ions recoiled from Si(111)-1×1-H by medium energy 80 – 150 keV Ne^+ impacts. The H^+ fraction is dependent on emerging angle and emerging energy. With decreasing the emerging angle scaled from the surface normal the H^+ fraction increases and reaches a saturation below ~ 70° and almost 100 % for emerging energy above 13 keV. In contrast, the charge state is not equilibrated even at ~85°. Such strong dependence on emerging angle is due to the location of H bound by Si atoms on top of the surface. The sensitivity to H on the surfaces is estimated to be better than 5×10^{12} atoms/cm^2 at a small emerging angle (θ_{out} < ~75°), where the H^+ fraction reaches ~100 %. The unexpectedly large energy spread for the recoiled H^+ spectra is attributed to the Doppler broadening caused by the zero-point energy of the vibrating H-Si system and additionally to small energy transfers among the three bodies of Ne^+ and H-Si, although the assumption of binary collision between Ne^+ and H is approximately valid. This H detection technique can be widely applied to analysis of chemical reactions including adsorption and desorption mediated by water and hydroxyl on various kinds of metal-oxide surfaces.

---

*Present address: *Department of Applied Quantum Physics and Nuclear Engineering, Kyushu University, 744 Motooka Nishi-ku, Fukuoka 819-0395, Japan*

1. Introduction

The role of H in materials science expands over many fields, including stabilization of dangling bonds in amorphous Si and Si_xGe_y films applied to solar cells and thin film transistors giving a positive effect, while H embrittlement of metals and deterioration of large scale integrated circuits (LSI) by inclusion of H result in a negative effect. It was also reported that H passivates the Si(111) and (001) surfaces by terminating the dangling bonds and keeps clean surfaces[1,2]. In catalysis, hydroxyl group (OH) plays an important role to enhance catalytic activities of metal clusters on metal oxides surfaces[3,4].

Variety of methods to detect H have been reported so far, induction coupled plasma, secondary ion mass spectrometry[5], elastic recoil detection analysis (ERDA)[6,7], nuclear resonant reactions[8,9] and electron stimulated emission[10]. Temperature programmed desorption combined with a quadrupole mass filter and infrared absorption analysis have been also employed to detect adsorbates containing H and vibrational modes of H bonds on surfaces, respectively. In traditional ion beam analysis, ERDA using MeV He^+ and heavy ions has been utilized to probe H in depth down to several hundred nm. In this case, an absorber foil is necessary to eliminate elastically scattered ions. Alternative ERDA techniques with time-of-flight detection[11-13] and combination of magnetic and electrostatic fields[14] have been also proposed.

Previously, we reported direct detection of H for Si(111)-1×1-H and hydroxylated TiO_2(110) surfaces using medium energy He^+ and Ne^+ ions[15]. This method was applied to the analysis of a gas phase CO oxidation on rutile TiO_2(110) surfaces[16], where the density of oxygen vacancies were determined by ERDA for the surface exposed to H_2O leading to paired OH formation. In this work, we first show strong dependence of a H^+ fraction on emerging angle and emerging energy for recoiled H from Si(111)-1×1-H surfaces. Detailed discussion is also made on the broadening of recoiled H^+ spectra considering the Doppler effect caused by the zero-point energy of the vibrating H-Si bond and other probable factors.

2. Experiment

We prepared carefully uniform Si(111)-1×1-H surfaces according to the methods recently proposed by Kato et al.[17] to obtain high quality surfaces and confirmed a clear 1×1 pattern by reflection high energy electron diffraction (RHEED). This method using

a 40 % w/w NH_4F buffered solution including $(NH_4)_2SO_3$ (1.0 % w/w) instead of an HF solution led to stronger water-repellency and more sharp 1×1 RHEED patterns than the usual treatment reported by Higashi et al.[18]. The key issue is to eliminate oxygen in the etching solution[17]. Therefore, we regard the surface as terminated completely by one monolayer (ML) of H (1 ML: 0.783×10^{15} atoms/cm^2).

Immediately after the surface treatment, the samples were introduced into an analysis chamber evacuated to an ultra high vacuum (~2×10^{-10} Torr). Ne^+ ions created in a duoplasma ion source were accelerated to 80 – 150 keV and collimated to a size of 0.18 mm in horizontal and of 2.0 mm in vertical planes before impinging on the samples mounted on a 6-axis goniometer. We measured precisely the beam current of ions incident on the samples which were positively biased by 90 V to suppress secondary electrons emission. The same bias voltage of +90 V was also applied to a final aperture placed 50 mm in front of the sample holder to absorb secondary electrons emitted from it. It is crucial to avoid the ion irradiation effect leading to decrease in areal H density on the Si(111) surface. Therefore, we utilized a low beam current of 1-2 nA and shifted slightly the beam position on the surface after a dose of 0.1 μC. The H ejection rate from the surface was evaluated quantitatively and the correction for the areal density of H on the surface was made to determine the H^+ fractions. A toroidal electrostatic analyzer (ESA) detected recoiled H^+ ions with an energy resolution (FWHM: full width at half maximum) of $\Delta E/E = 1 - 3\times10^{-3}$. Indeed, we estimated the energy resolution for 10 - 120 keV He^+ ions incident at 45° on Au(0.6 ML)/Ni(111) and scattered to 45° with respect to surface normal. The detailed discussion on the energy resolution will be made later in terms of the energy spread of recoiled H^+ profiles. The detection efficiency of the three-stage micro-channel plate coupled with a position sensitive detector attached to the toroidal ESA was measured in advance using 150 keV H^+ beams. From the scattering yield from Au of Ni(10.1 Å)/Au(4.0 Å)/Si(111) which was analyzed by Rutherford backscattering with 2.0 MeV He^+ ions, the detection efficiency was derived to be 0.44±0.02.

3. Results and Discussion

First we calculated numerically the cross sections for H recoiled by medium energy He^+, N^+ and Ne^+ incidence using the Ziegler-Biersack-Littmark (ZBL) potentials[19]. The calculated recoil cross sections for 100 keV He^+, N^+ and Ne^+ impact are shown in

Fig. 1. The recoil cross sections for N^+ and Ne^+ impacts are more than 2 orders of magnitude larger than for He^+ impact. It must be also noted that the above cross sections are 5 orders of magnitude larger than for MeV He^+ incidence[20]. Thus an excellent sensitivity to surface H is expected, if one uses medium energy Ne^+ ions.

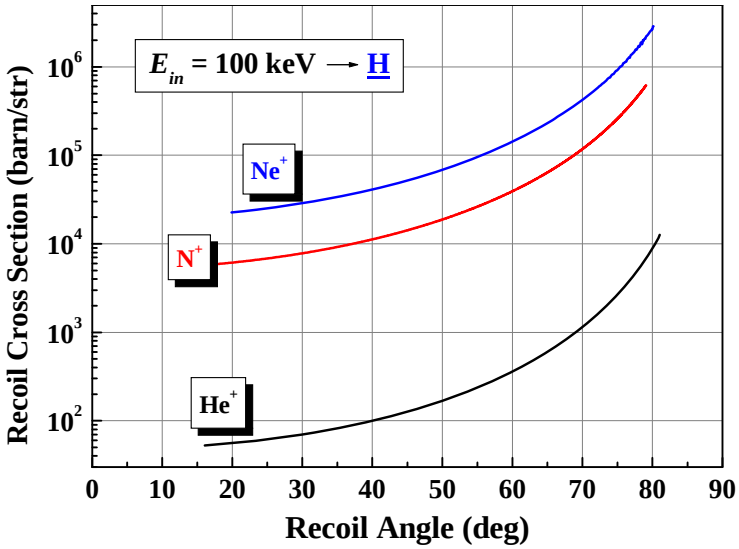

Fig. 1. Recoil cross sections calculated for 100 keV He^+, N^+ and Ne^+ impacts on H as a function of recoil angle using the ZBL potentials.

However, such high recoil cross sections may eject H significantly from the surface at a relatively small Ne^+ dose. We roughly estimate the total recoil cross section for medium energy Ne^+ impact on H at an impact parameter less than 1 Å. Note that the bond length of H-Si for Si(111)-1×1-H was derived to be 1.49 and 1.54 Å, respectively by the tight binding method[21] and first principles calculations[22]. If one assumes an unscreened Coulomb potential and an impact parameter (s) less than 1 Å, which result in ejection of H, the total recoil cross section (πs^2) is deduced to be 3.14×10^{-16} cm^2. This leads to H ejection of ~5 % after a Ne^+ dose of 0.1 μC. Actually we checked the H loss from the surface by Ne^+ impact by measuring the H^+ yields as a function of Ne^+ dose.

Figure 2 shows the H^+ yield for 143.9 keV Ne^+ impact on Si(111)-1×1-H at incident and emerging angles of 54.7 and 85.0°, respectively without shifting the irradiation area. The H^+ yield indicated at a dose of 0.1 μC, for example, means the data acquisition during Ne^+ irradiation from 0 to 0.1 μC. Unexpectedly, a strong H reduction takes place exponentially. The observed H^+ yield, $Y_H(I)$ is well reproduced by

$$Y_H(I) = Y_H(0)\exp[-I/\lambda], \quad (1)$$

where I is integrated beam current (μC), $Y_H(0) = 874.8$ and $\lambda = 0.372$ μC. This result indicates that ~25 % of H is lost from the surface after Ne^+ dose of 0.1 μC. Note that the data acquisition from 0 to 1 μC in this case corresponds to the recoil yield from the surface with an average H amount of 88 % of the initial value. The λ value is, of course, dependent on incident angle and Ne^+ energy. The data shown hereafter are after the correction of the H loss from the surface. As an additional contribution to H loss from the surface, we consider the sputtering effect and/or ion beam stimulated desorption like the electron stimulated desorption[10]. According to Matsunami et al.[23], the sputtering yield for 143.9 keV Ne^+ impact on Si is ~0.3, which leads to an H loss of ~6 % after a dose of 0.1 μC, if one assumes the same ejection rate for H as the sputter etching rate for Si. Therefore, the high ejection rate for H from the surface is probably due to the processes of recoil as well as sputtering and/or ion beam stimulated desorption.

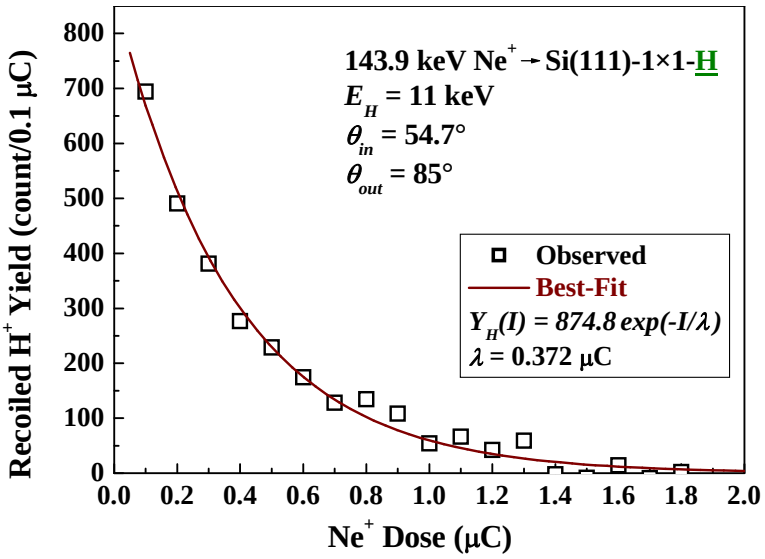

Fig. 2. H^+ yield (count per 0.1 μC) observed for 143.9 keV Ne^+ impact on Si(111)-1×1-H, as a function of Ne^+ dose (μC). The Ne^+ ions impinged on the same area of the surface during the measurement.

Now, we show a typical ERDA spectrum observed for 143.9 keV Ne^+ ions incident on the Si(111)-1×1-H at an angle of 58.0° (see Fig. 3). The H^+ ions recoiled to 72.5° with respect to surface normal were detected (recoil angle: ϕ = 49.5°). The recoiled H^+ spectrum was best-fitted by a symmetric Gaussian shape with FWHM of 213 eV, indicating no significant multiple scattering by underlying Si atoms. If we assume the

amount of H on the Si(111) to be just one monolayer, the H^+ fraction is deduced to be 79.0±7 %. As mentioned before, the H^+ fractions are dependent strongly on emerging angle and also significantly on emerging energy (the energy of H when emerging from the surface). The former is attributed to the location of H terminating the dangling bonds of the top layer Si atoms.

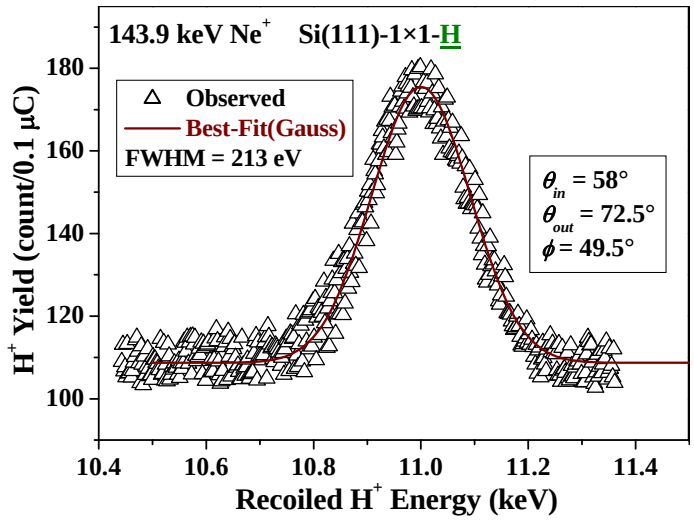

Fig. 3. Recoiled H^+ spectrum observed for 143.9 keV Ne^+ incidence on Si(111)-1×1-H. Incident and emerging angles scaled from surface normal are 58 and 70° (random), respectively. The spectrum was obtained by 5 point-smoothing (triangles) and best-fitted by symmetric Gaussian profile (solid curve).

Figures 4(a) and (b) indicate the singly-ionized fraction for H recoiled at 5 and 11 keV, respectively by 104.35 and 143.9 keV Ne^+ impacts, as a function of emerging angle which is scaled from the surface normal. The H^+ fraction abruptly increases with decreasing emerging angle and reaches saturated values of ~55 and ~88 % at an emerging angle below ~75° for recoil (emerging) energy of 5 and 11 keV, respectively. Such a high charge fraction reflects the fact that the H atoms bound to Si atoms are recoiled as H^+ (proton) in such a violent collision which accompanies a large energy transfer. The recoiled H^+ spectra become asymmetric with a tail on the lower energy side at an emerging angle above 87° owing to multiple scattering. The H^+ fraction seems still non-equilibrated even at an emerging angle more than 85°. Such a situation is ascribed to the location of the H terminating the dangling bond of the Si on top of the (111) surface, because the charge state of the recoiled H^+ is equilibrated via undergoing several times of electron capture and loss processes during passing through the surface

region[24]. Actually negatively charged H^- ions were not observed within the detection sensitivity even at emerging angles above 86° for recoil energy of 5 keV, although Marion-Young[25] predicted the equilibrium H^- fraction of ~5 %. The H^+ fraction saturated at a smaller emerging angle less than 75° is indicated in Fig. 5, as a function of emerging (recoil) energy. Interestingly, the H^+ fraction is saturated at 100 % for emerging angle of 13 keV.

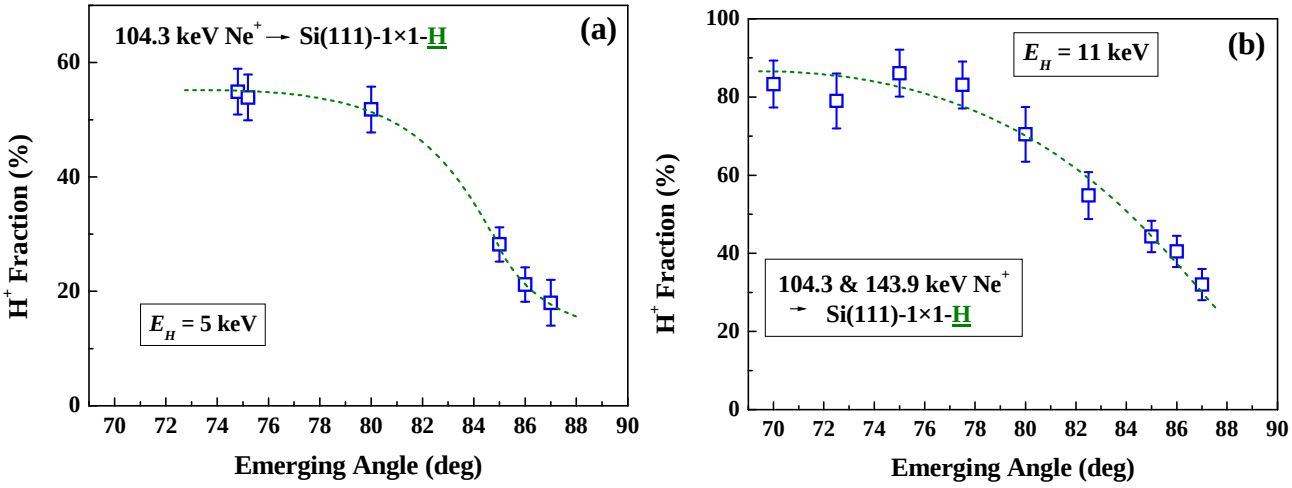

Fig. 4. Emerging angle dependent H^+ fractions for (a) 5 and (b) 11 keV H^+ ions recoiled by Ne^+ impacts. Dashed curves are drawn to guide the eyes.

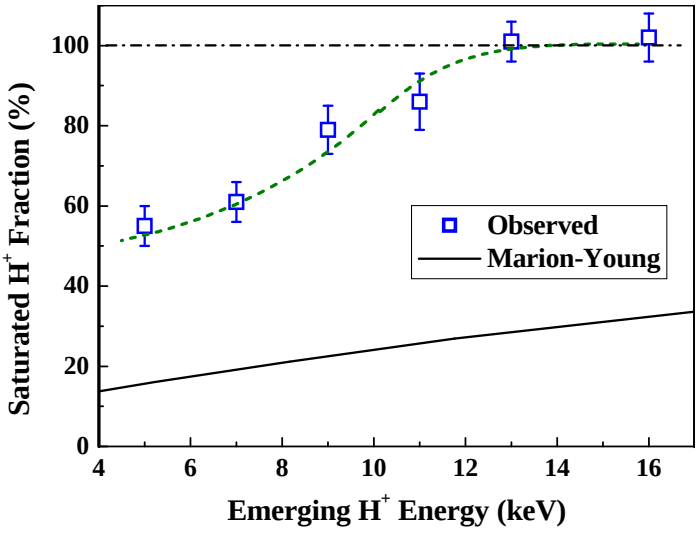

Fig. 5. H^+ fractions saturated at emerging angle around 70º, as a function of emerging energy. Solid curve corresponds to semi-empirical formula for equilibrium charge fraction of H^+ given by Marion-Young[25] and dashed curve is drawn to guide the eyes.

From the view point of the sensitivity, the H^+ detection at a smaller emerging angle is advantageous and the sensitivity to H is expected to be better than 5×10^{12} atoms/cm^2 for medium energy Ne^+ impact at a small emerging angle below ~75°. A larger recoil angle increases the recoil cross section but tends to result in multiple scattering and decreases the recoil (emerging) energy leading to a smaller H^+ fraction. Increase in emerging energy, however, enhances background level mainly originating from the components of Ne^+ scattered by Si and thus the optimum emerging angle and energy are ~75° and 10 - 13 keV, respectively. A similar situation probably takes place for detection of the H located on top of surfaces such a hydroxylated TiO_2(110) surface.

It is intriguing to elucidate the large energy spread of the recoiled H^+ spectra. Actually, such a large energy spread degrades the sensitivity of ERDA to H on the surface. There are some sources causing energy spreads of recoiled H^+ profiles, (i) system energy resolution including incident energy spread, a finite acceptance angle and energy resolution of the toroidal ESA, (ii) Doppler effect from the vibrating H-Si system and (iii) other unknown factors. Previously, we measured the energy resolution of the toroidal ESA by direct incidence of 60.0 keV He^+ ions and obtained a $\Delta E/E$ value (FWHM) of 9.0×10^{-4} [26]. The system energy resolution was estimated from the MEIS spectra observed in a wide range of 10 – 120 keV He^+ ions incident on Au(0.6 ML)/Ni(111) and scattered from Au. Here, 1 ML means an areal density of Ni(111)(1.86×10^{15} atoms/cm^2). The RHEED pattern observed for the Au/Ni(111) shows growth of two-dimensional (2D) Au(111) islands with the bulk Au-Au bond length of 2.88 Å (bulk Ni-Ni bond length is 2.49 Å). According to low energy ion scattering analysis[27], Au atoms are located on top of the surface and shifted by 0.3 Å toward the vacuum side from the top Ni(111) plane. Figure 6(a) is a typical MEIS spectrum for 10 keV He^+ incidence. The observed spectra were best-fitted by the exponentially modified Gaussian (EMG) line shape defined by

$$f(\Delta E)=\frac{1}{2\sigma_0}exp\{-\frac{1}{2\sigma_0}(2\Delta E-\frac{\sigma^2}{\sigma_0})\}\{1+erf(\frac{\Delta E-\sigma^2/\sigma_0}{\sqrt{2}\sigma})\}, \qquad (2)$$

where ΔE is a relative energy loss, *erf(x)* an error function, σ experimental system energy resolution, and σ_0 quantifying an asymmetry induced by a large-angle collision[28,29]. The spectrum rise and rear slope are fitted, respectively by assuming σ = 12.2 eV (standard deviation) and σ_0 = 34 eV. The energy resolution $\Delta E/E$ (FWHM) and the asymmetric factor σ_0 are indicated as a function of He^+ energy in

Figs. 6(b) and (c), respectively.

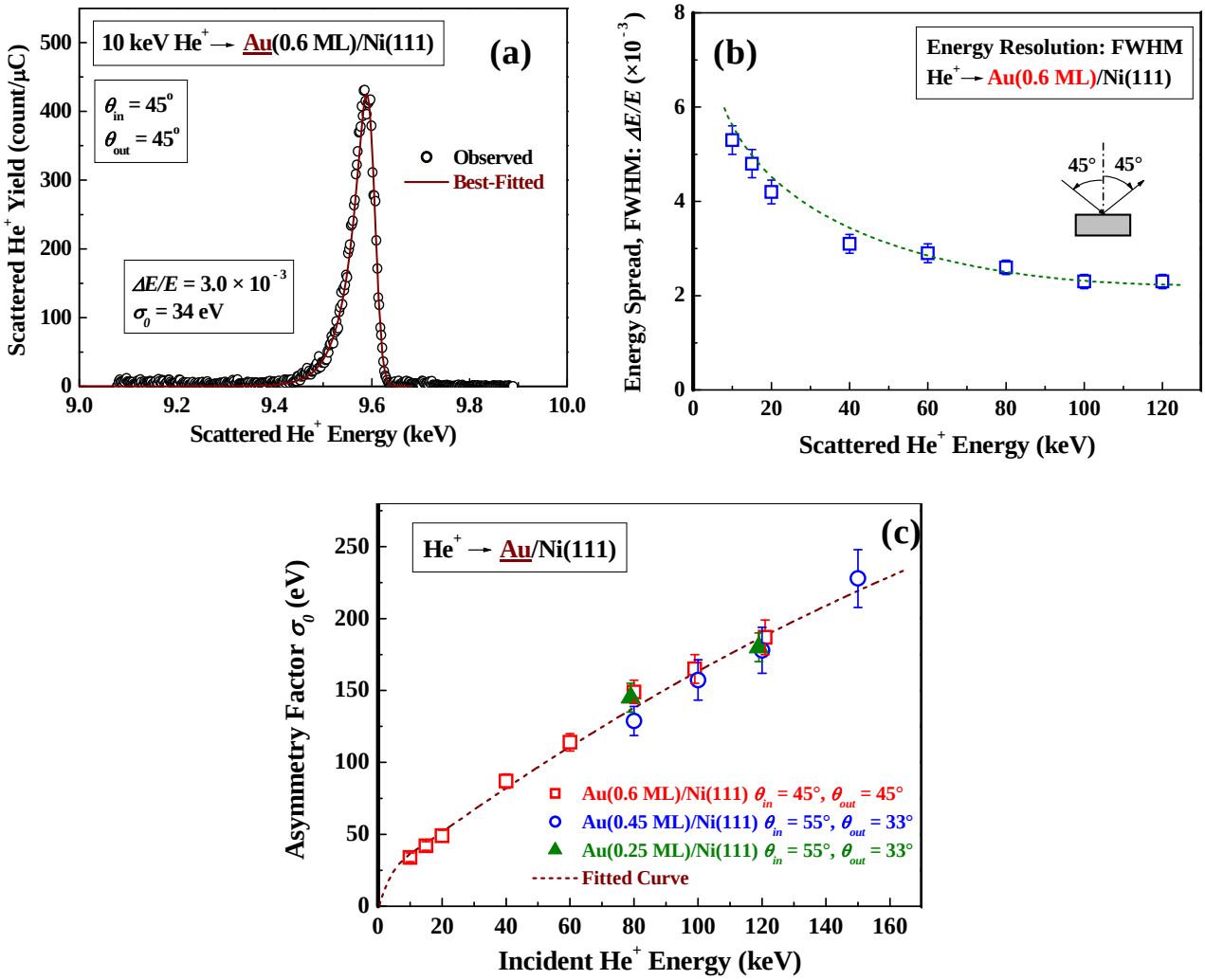

Fig. 6. (a) MEIS spectrum observed for 10 keV He^+ ions incident on Au(0.6 ML)/Ni(111) at 45° and scattered from Au to 45° with respect to surface normal. (b) System energy resolution of $\Delta E/E$ (FWHM) as a function of scattered He^+ energy. (c) Asymmetric factor σ_0 (eV) as a function of incident He^+ energy derived from best-fitting using EMG functions. The dashed curve is drawn to guide the eyes.

As the result, the contribution from the system energy resolution (FWHM) is ~33 eV for a recoil energy of 11 keV, which is negligibly small. It is interesting that the asymmetric factor σ_0 coming from inner shell excitations is well scaled almost linearly in a wide energy range from 10 up to 150 keV. This spectrum asymmetry becomes a crucial factor in best-fitting MEIS spectra from near-surface heavy atoms and also from nano-clusters of heavy metals[30]. Another factor to broaden the H^+ spectra is an

acceptance angle of the detector. The size of the aperture placed in front of the detector is 0.2 and 4.0 mm in the horizontal and vertical plane, respectively. A small variation of the recoil angle comes from a finite size in the horizontal plane, because recoiled H^+ ions are deflected in the horizontal plane. Considering the distance of 72 mm between the aperture and beam position on the sample surface, the acceptance angle is deduced to be 0.16°, which leads to an energy spread of ~30 eV for 125 keV Ne^+ incidence and recoil angle of 45°. Obviously this contribution to the energy spread is small enough.

Next, we estimate the contribution from the Doppler effect originating from the zero-point energy of the vibrating H-Si system. Based on the quantized harmonic oscillator model, if we take the momentum representation, the wave function of the system is given by

$$a_n(p) = \left(\frac{1}{\mu\omega\pi\hbar}\right)^{1/4} \frac{1}{\sqrt{2^n n!}} e^{-p^2/2\mu\omega\hbar} H_n(p/\sqrt{\mu\omega\hbar}), \qquad (2)$$

where μ, ω, $\hbar$, H_n are reduced mass, angular frequency, Planck constant and the Hermite polynomials of the n-th order, respectively and thus we obtain the velocity ($v = p/\mu$) distribution expressed as $|a_n(p)|^2$. According to high-resolution electron energy loss spectroscopy (HREELS)[17,31], the H-Si bending (lateral) and stretching (vertical) modes have the $\omega\hbar$ values of 78 and 258 meV, respectively, which are considerably larger than k_BT (k_B: Boltzmann constant) at room temperature (25 meV). Indeed, the probabilities to take the n = 1 state are estimated to be 0.046 and 3.3×10^{-5} for the bending and stretching modes, respectively at 300 K from the Planck distribution function. Therefore, we may well consider the zero-point energy ($\omega\hbar/2$) only and thus the velocity distribution is simply expressed by $\frac{1}{\sqrt{\mu\omega\pi\hbar}} exp(-\frac{\mu v_0^2}{\omega\hbar})$ (FWHM: $2\sqrt{ln2\omega\hbar/\mu}$). Figure 7 shows the energy spreads (FWHM) of H^+ recoiled at 11 keV estimated from the Doppler broadening due to the zero-point energy as a function of incident angle, which are compared with the observed ones. Obviously, the contribution from the Doppler broadening to the observed energy spread is 60-70 % at most, although significant correlation is seen on the incident angle dependence. The

situation is almost the same as that for different recoil energy. Fukutani et al.[9] detected the zero-point oscillation of the H-Si system using the nuclear resonant reaction of $^{1}H(^{15}N, \alpha\gamma)^{12}C$ at 6.385 MeV and derived the $\omega_{//}\hbar$ (bending mode) of 89 meV and $\omega_{\perp}\hbar$ (stretching mode) of 247 meV, which are consistent with the HREELS data. Note that this case satisfies the condition of a pure binary collision. In our case, however, small energy transfers may occur among the three bodies of Ne^{+} and H-Si, although the binary collision between Ne^{+} and H is approximately valid. In fact, the recoiled H^{+} profiles are almost symmetric Gaussian and the Monte Carlo simulations of ion-recoil trajectories reveals small enough events of multiple scattering from underlying Si atoms.

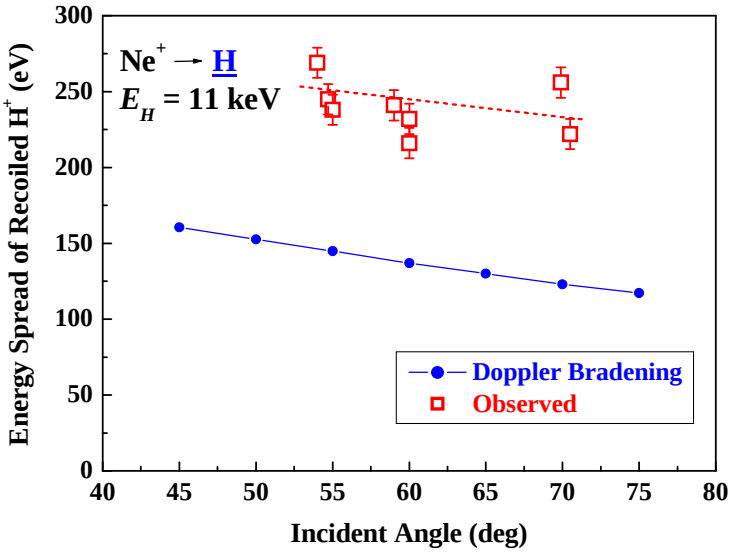

Fig. 7. Energy spread (FWHM) observed for H^{+} ions recoiled at 11 keV by Ne^{+} impact as a function of incident angle (open square). Full circles denote the contribution from the Doppler effect calculated assuming vibrating H-Si system with zero-point energy of 258/2 and 78/2 meV in the vertical and lateral directions, respectively.

5. Summary

It is shown that the elastic recoil detection of H using medium energy Ne^{+} impact gives an excellent sensitivity to surface H atoms better than 5×10^{12} atoms/cm^{2} for Si(111)-1×1-H surfaces. The recoiled H^{+} spectra are best-fitted by symmetric Gaussian shapes indicating no significant multiple scattering effect even at grazing emergence. The H^{+} fraction is dependent on emerging energy and strongly on emerging angle scaled from surface normal. The latter comes from the location of the H atoms bound to the top-layer Si. The H^{+} fraction reaches almost constant at emerging angle below ~75°

and 100 % for emerging energy above 13 keV, whereas the charge state equilibrium is not attained even at a large emerging angle above ~85°. The present result clearly indicates that the H is recoiled as a bared proton and then captures an electron with a low frequency. A careful check of H ejection from surfaces is required in order to obtain a good accuracy for the absolute amount of H located on top of the surfaces.

The unexpected large energy spread of recoiled H^+ spectra degrades the sensitivity. It is revealed that the Doppler broadening due to the zero-point energy of the vibrating H-Si system is the primary source to the energy spread but the contribution is 60-70 % at most. Another contribution probably comes from a small energy transfer between Ne^+ and H-Si system during the recoil process. However, the binary collision model for the Ne^+-H system is approximately valid, because the recoiled H^+ spectra take almost symmetric Gaussian shapes and the Monte Carlo simulations of ion-recoil trajectories reveals negligibly small probabilities for the multiple scattering from underlying Si atoms.

It is not clear at present that this method makes it possible to give depth profiles of H with a good depth resolution and sensitivity. We expect, however, that taking a glancing incidence geometry may allow for depth profiling, although the probing depth is probably limited to less than ~10 ML owing to recoil energy broadening. Despite that, this technique can be widely applied to analysis of surface electrochemistry including adsorption and desorption mediated by water and hydroxyl on various kinds of metal-oxides surfaces[32,33].

Acknowledgements

The authors would like to appreciate H. Yamada and M. Arizono for their assistance in the present ERDA experiments. This work was carried out under the supports of Japan Science and Technology Agency, JST, CREST and Ministry of Education, Japan, ‘Academic Frontier Project’.

References

[1] Y.J. Chabal and K. Raghavachari, Phys. Rev. Lett. **53**, 282 (1984).

[2] T. Takahagi, I. Nagai, A. Ishitani, and H. Kuroda, J. Appl. Phys. 64, 3516 (1988).

[3] Y. Du, N.A. Deskins, Z. Zhang, Z. Dohnálek, M. Dupuis, I. Lyubinetsky, Phys. Rev. Lett. **102** (2009) 096102.

[4] J. Matthiesen, S. Wendt, J.Ø. Hansen, G.K.H. Madesen, E. Lira, P. Galliker, E.K. Vestergaard, R. Schaub, E. Lægsgaard, B. Hammer, and F. Besenbacher, ACS, Nano **3** (2009) 517.

[5] A. Benninghoven, K.-H. Müller, C. Plog, M. Schemmer, and P. Steffens, Surf. Sci. **63**, 403 (1977).

[6] J.E.E. Baglin, A.J. Kellock, M.A. Crockett, A.H. Shin, Nucl. Instrum. Methods **B 64** (1992) 469.

[7]. A. Mikami, T. Takagawa, K. Nishio, H. Ogawa, T. Okazawa, and Y. Kido, Appl. Surf. Sci. **252** (2006) 5124.

[8] Y. Iwata, F. Fujimoto, E. Vilalta, A. Ootuka, K. Komaki, K. Kobayashi, H. Yamashita, and Y. Murata, Nucl. Instrum. Methods **B 33** (1988) 574.

[9] K. Fukutani, A. Itoh, M. Wilde, M. Matsumoto, Phys. Rev. Lett. **88** (2002) 116101.

[10] K. Ueda, S. Kodama, and A. Takano, Surf. Sci. **283** (1993) 195.

[11] M. Copel and R.M. Tromp, Rev. Sci. Instrum. **64** (1993) 3147.

[12] F. Shoji, A. Yamada, T. Shiramizu, and K. Oura, Nucl. Instrum. Methods **B 135** (1998) 366.

[13] G. Dollinger, A. Bergmaier, L. Goergens, P. Neumaier, W. Vandervorst, and S. Jakschik, Nucl. Instrum. Methods **B 219-220** (2004) 333.

[14] K. Kimura, K. Nakajima, and H. Imura, Nucl. Instrum. Methods **B 140**, 397 (1998).

[15] K. Mitsuhara, T. Kushida, H. Okumura, H. Matsumoto, A. Visikovskiy and Y. Kido, Surf. Sci. **604** (2010) L48.

[16] K. Mitsuhara, F. Matsuda, H. Okumura, A. Visikovskiy, and Y. Kido, Nucl. Instrum. Methods **B 269** (2011) 1859.

[17] H. Kato, T. Taoka, S. Nishikata, G. Sazaki, T. Yamada, R. Czajka, A. Wawro, K. Nakajima, A. Kasuya and S. Suto, Jpn. J. Appl. Phys. **46** (2007) 5701.

[18] G.S. Higashi, R.S. Becker, Y.J. Chabal, and A.J. Becker, Appl. Phys. Lett. **58**, 1656

(1991).
[19] J.F. Ziegler, J.P. Biersack, and W. Littmark, *The Stopping and Range of Ions in Matter* (Pergamon, New York, 1985).
[20] A. Mikami, T. Takagawa, K. Nishio, H. Ogawa, T. Okazawa and Y. Kido, Appl. Surf. Sci. **252** (2006) 5124.
[21] B.J. Min, Y.H. Lee, C.Z. Wang, C.T. Chan and K.M. Ho, Phys. Rev. **B 45** (1992) 6839.
[22] E. Kaxiras and J.D. Joannopoulos, Phys. Rev. **B 37** (1988) 8842.
[23] N. Matsunami, Y. Yamamura, Y. Itikawa, N. Itoh, Y. Kazumata, S. Miyagawa, K. Morita, R. Shimizu and H. Tawara, Atom. Data and Nucl. Data Tables **31** (1984) 1.
[24] Y. Kitsudo, K. Shibuya, T. Nishimura Y. Hoshino, I. Vickridge and Y. Kido, Nucl. Instrum. Methods **B 267** (2009) 566.
[25] J.B. Marion and F.C. Young, *Nuclear Reaction Analysis – Graphs and Tables* (North-Holland, Amsterdam, 1968).
[26] Y. Kido, T. Nishimura, Y. Hoshino and H. Namba, Nucl. Instrum. Methods **B 161-163** (2000) 371-376.
[27] K. Umezawa, S. nakanishi and W.M. Gibson, Surf. Sci. **426** (1999) 225.
[28] P.L. Grande, A. Hentz, R.P.Pezzi, I.J.R. Baumvol, G. Schiwietz, Nucl. Instrum. Methods **B 256** (2007) 92.
[29] M. Hazama, Y. Kitsudo, T. Nishimura, Y. Hoshino, P.L. Grande, G. Schiwietz and Y. Kido, Phys. Rev. **B 78** (2008) 193402(1-4).
[30] M.A. Sortica, P.L. Grande, G. Machado and L. Miotti, J. Appl. Phys. 106 (2009) 114320.
[31] Ch. Stuhlmann, G. Bogdányi and H. Ibach, Phys. Rev. **B 45** (1992) 6786.
[32] Z. Dohnálek, I. Lyubinetsky and R. Rousseau, Prog. Surf. Sci. **85** (2010) 161.
[33] K. Mitsuhara, T. Matsuda, H. Okumura, A. Visikovskiy and Y. Kido, Nucl. Instrum. Methods **B 269** (2011) 1859.